ELSEVIER

Neurobiology of Aging 21 (2000) 349–355

NEUROBIOLOGY OF AGING

www.elsevier.com/locate/neuaging

Agrin and microvascular damage in Alzheimer's disease

Tyler M. Berzin[a], Brian D. Zipser[a], Michael S. Rafii[b], Victoria Kuo—Leblanc[a], George D. Yancopoulos[c], David J. Glass[c], Justin R. Fallon[b], Edward G. Stopa[a,d,*]

[a]*Department of Pathology (Neuropathology Division), Brown University, Rhode Island Hospital, 593 Eddy Street, Providence, RI 02903 USA*
[b]*Department of Neuroscience, Brown University, Providence, RI, 02912 USA*
[c]*Regeneron Pharmaceuticals, Inc., 777 Old Saw Mill River Road, Tarrytown, NY, 10591 USA*
[d]*Human Brain Tissue Resource Center, McLean Hospital/Harvard Medical School, Belmont, MA 02178*

Received 22 October 1999; received in revised form 25 January 2000; accepted 31 January 2000

Abstract

Heparan sulfate proteoglycans (HSPGs) are ubiquitously present within the perivascular basement membrane, and have been shown to be altered in patients with Alzheimer's Disease (AD). Although the HSPG agrin clearly orchestrates the differentiation of the neuromuscular junction, its role in the brain remains unclear. Growing evidence suggests that agrin may be an important vascular basement membrane (VBM)-associated HSPG. In previous studies, we demonstrated that agrin is present throughout the brain microvasculature, as well as in neuronal cell bodies. AD brains exhibited fragmentation of VBM-associated agrin. Agrin immunoreactivity was also seen within senile plaques and neurofibrillary tangles. These changes were accompanied by the appearance of an additional pool of insoluble agrin. In the present study, we provide further evidence for microvascular damage in AD, by examining the distribution of agrin and laminin within the VBM, and by measuring the agrin concentration within hippocampus and prefrontal cortex. Furthermore, we assessed blood-brain-barrier (BBB) leakage by examining the perivascular distribution of prothrombin immunoreactivity. Soluble agrin levels were increased approximately 30% in Braak stage III–VI AD patients relative to age-matched controls. Furthermore, agrin and laminin exhibited identical patterns of VBM fragmentation in AD and colocalized with beta-amyloid in senile plaques. Microvascular changes were associated with the appearance of perivascular prothrombin immunoreactivity. Our data suggest that agrin is an important VBM-associated HSPG in the brain and that agrin levels are altered in association with microvascular damage in AD.

Keywords: Agrin; Alzheimer's Disease; Heparan sulfate proteoglycans; Vascular basement membrane; Blood–brain barrier; Laminin; Prothrombin

1. Introduction

Alzheimer's Disease is characterized by loss of short-term memory and cognitive abilities, ultimately leading to more severe dementia, unresponsiveness, and death [37]. Although senile plaques and neurofibrillary tangles are the neuropathological hallmarks of AD, significant microvascular pathology including reduced vascular density, atrophic vessels, and vascular amyloid deposits have also been described in AD [5,34].

Several studies have shown correlations between the distribution of HSPGs and the distribution of the characteristic lesions of AD [35,42]. Evidence suggests that HSPGs may be directly involved in the formation and/or persistence of amyloid plaques [43]. Moreover, the amyloid precursor protein (APP) binds heparan sulfate, suggesting that the interaction of APP with HSPG in the extracellular matrix may stimulate the effects of APP on neurite outgrowth [39]. It has been suggested that APP-proteoglycan interactions may disturb normal APP function and contribute to the neuritic outgrowth surrounding the cores of senile plaques [40]. Our most recent study demonstrated that the VBM-associated HSPG agrin is also present in AD neuropathological lesions [13].

Agrin is a large, multidomain heparan sulfate proteoglycan [44] that was first isolated from the basal laminae of the Torpedo electric organ. It was identified by its ability to organize the aggregation of myoblast acetylcholine receptors and other postsynaptic elements beneath the nerve terminal [31,36, 45]. More recent studies have demonstrated the existence of several isoforms of the protein with differing specificity and signaling capabilities [3]. In studies of the rat and chick ner-

* Corresponding author. Tel.: +1-401-444-5057; fax: +1-401-444-8514.
E-mail address: edward_stopa@brown.edu (E.G. Stopa).

0197-4580/00/$ – see front matter
PII: S0197-4580(00)00121-4

vous systems, agrin was found to be a component of all basal laminae, both at the more extensively studied neuromuscular junction and within the brain [41,8,18]. Agrin's presence in the CNS, including the brain and retina, suggests that it may be required for synapse formation there as well. This possibility is supported by evidence that agrin mRNA in the brain is most highly expressed during developmental stages associated with synapse formation as well as in brain areas exhibiting high synaptic plasticity [22,2].

Of particular interest to this study is the finding that agrin is found extensively in the basal lamina of the brain microvasculature [1]. It is thought that the basis of agrin's localization in basement membranes may be its binding, at the amino terminus, with the extracellular matrix molecule, laminin [12]. We previously described the presence of agrin in neurons and the microvascular basal lamina of normal human brains. In AD brains, we noted that the solubility properties of agrin were significantly altered due to the appearance of SDS-insoluble agrin. Furthermore, we noted that agrin immunoreactivity was characterized by a punctate staining pattern closely associated with both neuritic plaques and adjacent blood vessels. Almost without exception, the blood vessels within or adjacent to agrin deposits were characterized by attenuated diameters and irregular-looking vascular walls.

Considering this widespread alteration in microvascular appearance in AD, we hypothesized that AD patients may have increased BBB permeability, resulting in increased serum protein accumulation within the brain extracellular space. We therefore decided to investigate whether microvascular damage could be identified by perivascular prothrombin immunoreactivity. Prothrombin is the 72 kDa plasma proenzyme of thrombin involved in the coagulation cascade. Although prothrombin is also produced by neurons, it has been used in previous CNS studies as an indicator of BBB leakage [15]. The ratio of prothrombin in the CSF to plasma protein concentration was previously correlated to the CSF albumin/plasma protein ratio, which has also been used as an indicator of basal membrane permeability [28].

Considering that agrin's distribution in AD brains parallels the neuropathological lesions of the disease, we sought to characterize more precisely the nature of agrin deposits by comparing agrin's distribution to that of amyloid and laminin. We chose to examine amyloid for its obvious importance in AD, and laminin because it is an important basal lamina component that is thought to bind both agrin and amyloid [30,12]. Finally, given the abundance of agrin immunoreactivity in AD brains, we sought to quantify the levels of soluble agrin in AD brains relative to controls.

2. Materials and methods

2.1. Human tissues

All brains were obtained at autopsy (postmortem interval 2–24 h). Fourteen brain areas were routinely sampled in our protocol. These representative areas were carefully selected on the basis of their suitability for diagnosing AD, as well as the other currently classified neurodegenerative diseases. The diagnosis of AD was made in accordance with widely accepted National Institute of Aging criteria [24], as well as the Braak neuropathological staging of Alzheimer-related changes [4]. Control brains were obtained from aged hospital patients with no history of neurological disease and no pathologic evidence of AD or other degenerative brain diseases (Table 1).

Table 1.
Clinical summary of autopsy cases

	AD-Braak stage	Age	Sex	PMI*	Cause of death
1	Control	60	M	12	Colon CA
2	Control	66	F	14	Breast CA
3	Control	70	F	3.5	CHF, pulmonary hemorrhage
4	Control	71	M	17	Vehicular trauma
5	Control	62	F	17.5	ARDS
6	Control	63	M	19	Lung CA
7	Control	75	M	23	Drowning
8	Control	82	F	9	Adenocarcinoma (pancreas)
9	Control	85	F	21.5	Cardiac arrest, CAD
10	Control	82	M	24	Cardiac arrest, CAD
11	Control	51	M	24	MI
12	Control	77	M	13	MI, diabetes
13	I-II	82	F	13	Cardiac arrest
14	I-II	76	M	18	Lymphoma
15	I-II	61	M	15	Lung CA
16	I-II	78	F	11	Cardiac arrest
17	I-II	79	F	20	Cerebral atrophy
18	I-II	91	M	20	Pneumonia
19	I-II	67	F	16	COPD
20	I-II	87	M	23	Renal failure
21	I-II	70	F	21	Metastatic lung CA
22	III-IV	83	F	6	Cardiac arrest
23	III-IV	68	F	9.5	Cardiac arrest
24	III-IV	78	M	9.5	MI
25	III-IV	77	F	18	Pneumonia
26	III-IV	74	M	13	CHF
27	III-IV	80	M	17	CHF
28	III-IV	75	M	6	S/P CABG
29	V-VI	73	M	18	Pneumonia
30	V-VI	73	M	13	Pneumonia
31	V-VI	66	F	2	Cardiac arrest
32	V-VI	87	F	12.5	Renal failure
33	V-VI	77	M	9.2	Pneumonia
34	V-VI	79	F	5	Aortic Aneurysm
35	V-VI	87	F	19.5	Cardiac arrest

* Postmortem interval (hrs).

Abbreviations: ARDS—adult respiratory distress syndrome; AD—Alzheimer's disease; CABG—coronary artery bypass graft; CAD—coronary artery disease; CHF—congestive heart failure; COPD—chronic obstructive pulmonary disease; MI—myocardial infarction; S/P—status post.

2.2. Immunohistochemistry

Samples of prefrontal cortex (Broadmann A10) and hippocampus were fixed by immersion in 4% paraformal-

dehyde in 0.1 M phosphate buffer (pH 7.4) for 24 h. and cryoprotected with 30% sucrose in 0.1 M phosphate buffer (pH 7.4). Samples were then snap-frozen in liquid nitrogen and stored at −70°C until used. For agrin immunostaining, an anti-human agrin antisera (#F60605I) was raised in rabbits by immunization with a recombinant C-terminal 50kDa fragment of agrin 4,8 produced in *Pichia pastoris* comprising the G2 and G3 domains [14]. Unlike other anti-agrin antibodies that selectively bind neuronal agrin [8] or endothelial agrin [1], our anti-agrin antibody has a broad specificity, revealing both neuronal and microvascular immunoreactivity. Frozen tissue samples were embedded in OCT and sectioned at a thickness of 8 μm and mounted on glass slides. The tissue was pretreated with 3% hydrogen peroxide and 10% normal goat serum. After pretreatment, tissue sections were incubated in the polyclonal anti-human agrin antibody. For the amyloid, co-localization study, tissue samples were incubated with both the anti-agrin antibody and a monoclonal anti-beta amyloid antibody (6E10, Boehringer Manheim, Indianapolis, IN, USA). After 24–48 h of incubation in primary antisera, tissue sections were washed and incubated in a goat anti-rabbit Ig conjugated to CY3 (Jackson), and a goat-anti-mouse Ig conjugated to FITC (Jackson). To eliminate autofluorescence from tissue lipofuscin, sections were post-treated with 0.3% Sudan Black B in 70% ethanol for 10 min before being washed in distilled water. Slides were then coverslipped using Permafluor aqueous mounting medium.

A second procedure was used to examine the comparative distribution of laminin and agrin. Tissue sections were incubated in polyclonal anti-laminin antibody (Sigma Chemical Co., St. Louis, MO, USA), whereas directly adjacent sections were incubated in polyclonal anti-agrin antibody. After washing and incubation in goat anti-rabbit CY3 (for agrin) and goat anti-rabbit FITC (for laminin), the protocol was completed using the previously described procedure to eliminate autofluorescence. The specificity of the anti-agrin antibody was confirmed on human brain and muscle sections as previously described [13].

For the anti-prothrombin studies, frozen tissue sections were prepared as described above. Tissue samples were pretreated with an endogenous peroxidase block by incubation in 0.3% H_2O_2 followed by incubation in 10% normal rabbit serum. Tissues were exposed to primary antibody for 18–24 h in a 1:500 dilution of goat anti-human prothrombin (ICN Biomedicals). The sections were washed and then incubated in a 1:100 dilution of FITC conjugated rabbit anti-goat IgG for 2 h. Slides were then coverslipped as described above.

2.3. ELISA assays

In addition to immunohistochemical localization studies, the protein concentration of soluble agrin was measured by ELISA analysis in both the hippocampus (controls, $N = 12$; AD, $N = 23$) and the prefrontal cortex (controls, $N = 10$; AD, $N = 12$). Samples of brain tissue were snap frozen in liquid nitrogen and ground into powder. The powder was transferred to disposable 10-ml conical microtubes and combined with the homogenization buffer consisting of 20 mM Tris-HCL, pH 7.4; 2.0M NaCl; 1 mM EDTA; 1 mM EGTA; 0.5% Deoxycholate; 1% Igepal; proteinase inhibitor cocktail (1 mM PMSF and 1μg/ml of each of the following: Aprotinin, Leupeptin, Pepstatin A). After sonication for 1 min and centrifugation at 14 000 rpm for 30 min at 4°C, the total protein content of clarified supernatants was determined by assay kits from Pierce (Rockford, IL, USA; catalog 23224).

For determination of agrin concentration, the Pierce ELISA protocol was used in accordance with the manufacturer's instructions. An ELISA plate was incubated overnight at 4°C with 1 mg/ml anti-agrin antibody in carbonate/bicarbonate buffer, pH 9.6. The plate was then washed 1× (Kierkegard and Perry Wash Solution; Gaithersburg, MD, USA) and BSA was added at a concentration of 1/10. After 1 h of room temperature (RT) incubation, the plate was again washed. Standards and samples were prepared in 1/15 BSA and added to the wells. After 2 h of incubation at RT, the plate was washed and 100 ml of biotinylated anti-agrin antibody was added per well at a concentration of 50 ng/ml in 1/15 BSA. The plate was incubated at 37°C for 1 h. After another wash step, 100 ml of Avidin D was added per well (1/1000 in 1/15 BSA). The reaction was incubated for 1 h at RT. Following the wash step, 100 ml of TMB solution was added to each well. After 20 min the reaction was stopped with 1M Phosphoric Acid, and the plate was read at a wavelength of 492 nm.

3. Results

3.1. Comparative distribution of agrin and beta amyloid

A double-labeling immunofluorescence procedure was used to compare the distributions of agrin and amyloid. In each AD tissue sample, the agrin antibody labeled all amyloid-containing structures including plaques (agrin, Fig. 1A; amyloid Fig. 1B) and neurofibrillary tangles. Within most plaques, there were distinct differences between agrin and amyloid labeling. Although agrin labeling was distributed in a punctate fashion within each plaque and around microvessels, amyloid labeling was more homogeneous. Additionally, the anti-agrin antibody labeled all microvascular basement membranes (Fig. 1C).

3.2. Distribution of prothrombin in AD and control

An immunofluorescence comparison of the Alzheimer's sections and the normal aged control sections revealed an increase in perivascular prothrombin immunoreactivity in

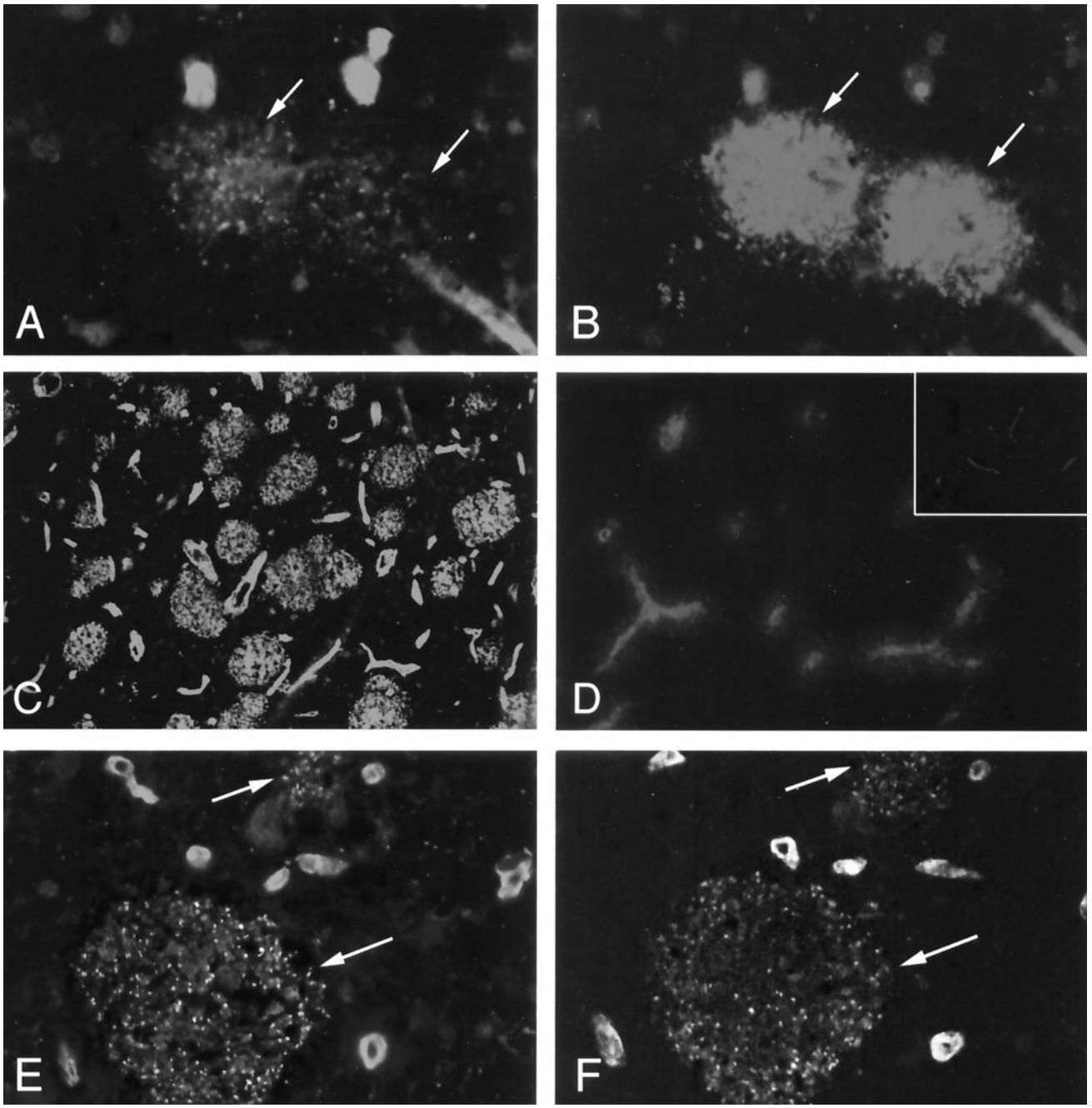

Fig. 1. A, high magnification of AD hippocampus illustrating two neuritic plaques (arrows). Puncta are clearly evident throughout the plaque and an associated blood vessel is evident at lower right. 600 ×. B, the same section of AD hippocampus as A, shown here with FITC-labeled anti-amyloid immunoreactivity. Amyloid staining is more homogeneous. This is especially true near the center of the plaque, whereas there are more puncta peripherally. 600 ×. C, amygdala of a patient with AD, labeled with anti-agrin antibody. Note the robust staining of neuritic and diffuse plaques and blood vessels. Blood vessels in this AD case have attenuated diameters and ragged profiles. 200 ×. D, prothrombin immunoreactivity in AD prefrontal cortex. Note the appearance of perivascular prothrombin immunoreactivity and an increase in background staining relative to a normal aged control (inset). 400×. E, Amygdala of a patient with AD, labeled with anti-agrin antibody (CY3 fluorescence). Clear punctate immunoreactivity is evident in the two plaques, both marked with arrows. 600 ×. F, adjacent tissue section of AD amygdala shown in 1e, with FITC-labeled anti-laminin immunoreactivity. Once again, anti-laminin antibody labels both plaques. Laminin immunoreactivity is also notably punctate and displays a staining pattern remarkably similar to agrin distribution. Anti-laminin antibody also robustly labels surrounding blood vessels, several of which are shown in cross section. 600 ×.

the AD tissue. AD sections also exhibited a brighter background distribution of prothrombin (Fig. 1D). No such accumulations of prothrombin were identified in the normal aged cases (Fig. 1D, inset).

3.3. Comparative distribution of agrin and laminin

Agrin and laminin exhibited an identical distribution of reaction product (adjacent sections, Fig. 1E and F), labeling

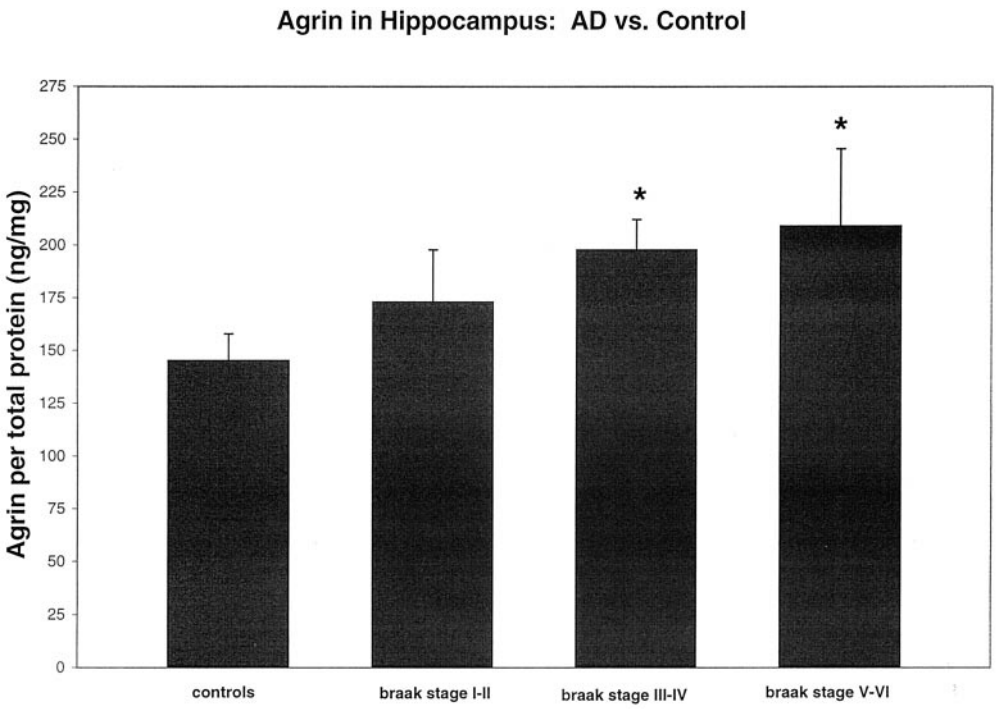

Fig. 2. Nanograms of soluble agrin per milligrams total protein in control and AD brains. Soluble agrin levels were measured by quantitative ELISA. Values are mean ± SEM. * Both Braak III–IV and V–VI brains had significantly more soluble agrin per milligram total protein than control brains, $P < 0.01$, Student's *t*-test.

plaques and microvessels in AD brain tissue. Plaque staining for both agrin (Fig. 1E) and laminin (Fig. 1F) was characterized by punctate immunoreactivity. The similarity of plaque-associated immunoreactivity to the pattern seen around individual microvessels, as well as the close proximity between plaques and microvessels, suggested that the plaque-associated agrin and laminin may originate from the VBM.

3.4. ELISA analysis

Control and AD samples of hippocampus and prefrontal cortex (A10) were analyzed for the nanogram concentration of soluble agrin per mg total protein. AD samples were separated into three subgroups based on Braak and Braak staging (I–II, III–IV, and V–VI). In control hippocampus ($N = 12$) the ng agrin/total mg protein average was 145.2 ng/mg. In AD hippocampus, the ng agrin/total mg protein varied according to disease severity. Braak stage I–II hippocampus ($N = 9$) had an average agrin level of 172.9 ng/mg. In Braak stage III–IV ($N = 7$) the value was 197.7 ng/mg, and in Braak stage V–VI hippocampus ($N = 7$), the value was 209.3 ng/mg (Fig. 2). Our prefrontal cortex experiment compared controls ($N = 9$) with Braak stage V–VI brains ($N = 12$) and yielded similar results. The amount of soluble agrin per total protein in control A10 was 151.1 ng/mg. This number increased to 187.7 ng/mg for the Braak stage V–VI brains. The Braak stage I-II brains did not show a statistically significant increase in agrin levels when compared to controls ($P > 0.05$, Student-*t* test). However, the Braak stage III-IV and V-VI brains showed a statistically significant increase in soluble agrin levels as compared to controls ($P < 0.001$).

4. Discussion

Growing evidence suggests that microvascular damage may be a significant factor in the pathogenesis of Alzheimer's disease. Our results show increased prothrombin immunoreactivity around the microvasculature and elevated background levels of prothrombin, most probably the result of blood-brain-barrier disruption. We also explored the possibility of microvascular basement membrane alteration in AD, by comparing agrin's distribution with that of laminin, an extracellular matrix protein that is found chiefly in the basement membrane of cerebral blood vessels.

Our results demonstrate that anti-laminin and anti-agrin immunoreactivity in plaques is identical, both in distribution and in overall appearance. This suggests that the agrin present in plaques is directly associated with the microvascular basement membrane. This finding supports previous reports that all plaques are closely associated with blood vessels, implicating microvascular degeneration as a primary event in the pathogenesis of Alzheimer's Disease [33].

In previous experiments, we noted that agrin immunoreactivity was altered in AD brains, and that there was a shift in the solubility properties of agrin due to an increase in the

amount of amyloid-associated SDS-insoluble agrin. The distribution of agrin immunoreactivity seemed to coincide with the amyloid-containing senile plaques and neurofibrillary tangles. On Western analysis, agrin was readily solubilized in control brains, whereas AD brains exhibited both soluble and insoluble fractions. In this study we attempted to quantify the amount of soluble agrin in AD and control brains. Our ELISA results show a significant increase in soluble brain agrin in moderate/severe AD hippocampus and prefrontal cortex relative to controls. This finding could have several different explanations as our anti-agrin antibody does not differentiate between neuronal and non-neuronal isoforms of agrin. The agrin isoform derived from non-neural cells lacks a 4 amino acid insert that is known to be required to induce AChR clustering. Due to mRNA splicing, neurons secrete a number of different agrin isoforms with varying ability to induce AChR aggregation [32].

We previously hypothesized that the apparent increase in neuronal agrin immunoreactivity that we observed in AD may reflect the abnormalities in synaptic structure and function, which are the earliest manifestations of AD pathology [9,20]. These changes precede both the deposition of extracellular fibrillar beta amyloid and the accumulation of APP within neurites, astrocytes, and microglia. It is possible that our ELISA results reflect an increase in neuronal agrin, perhaps reflecting synaptic changes and/or the adaptive growth responses that may accompany degenerative events in diseased brain [16]. Indeed, agrin is required for presynaptic differentiation at nerve-muscle synapses [6] and may play a role in axonal outgrowth in the CNS [18]. Thus, agrin could potentially function in the characteristic neuritic sprouting observed in AD [26]. Given the AChR clustering ability of the neuronal isoform of agrin, it is tempting to speculate that neuronal agrin could serve as an organizer of plaque formation. Furthermore, the recent identification of an agrin receptor in cortical neurons as well as agrin's calcium-dependent regulation of c-fos makes agrin's potential role in AD even more intriguing [21]. Indeed, neuronal c-fos is known to be upregulated in AD [46].

Given the ubiquitous presence of agrin immunoreactivity in the vascular basal lamina, as well as the striking alterations in microvasculature associated with AD lesions, it seems more likely that our ELISA results reflect microvascular alterations associated with AD rather than neuronal alterations. Furthermore, previous findings indicate that in the CNS the predominant agrin isoform is that which is secreted predominantly by non-neural cells and lacks strong AChR clustering ability [32]. This does not eliminate the possibility of quantitative alterations in neuronal agrin, but it is likely that such changes may be overshadowed by the sheer abundance of agrin in the vascular basal lamina.

The dramatic alteration in microvascular agrin is important for several reasons. Components of the extracellular matrix may regulate blood–brain-barrier (BBB) breakdown via regulation of tissue proteases and related factors. Further, agrin could serve as a coordinator of interactions between basement membrane and amyloid, leading to AD degeneration. Vascular fragmentation may result in widespread agrin deposition, which could facilitate beta-amyloid fibril deposition due to agrin's glycosaminoglycan chains [7]. Further, the recent discovery of the cortical agrin receptor also revealed that all alternatively spliced forms of agrin are equally capable of inducing c-fos expression [21]. Thus, the widespread agrin deposition characteristic of AD is particularly revealing in light of agrin's potential effects on neuronal gene regulation.

The vascular degeneration hypothesis may also be linked to ApoE genotype, as ApoE has been implicated as a predictor of vascular integrity [23]. In fact, individuals with the ApoE4 allele (a risk factor for the development of AD) are also predisposed to vascular dementia and other vascular diseases [29]. It is worth noting that agrin deposits may simply be a symptom of microvascular damage— which itself may impair cerebral metabolism, possibly leading to the degenerative events of AD [11]. Agrin is, however, well-positioned to play a role in Alzheimer's disease pathology. The dramatic agrin alterations observed in AD could modify synaptic structure and plasticity, promote the aggregation of beta amyloid, or modulate some other aspect of neuronal function. Our results support the notion that there is significant microvascular damage in AD and raise the possibility that the AD-related alterations in the distribution and quantity of the HSPG agrin may regulate interactions between amyloid and the basement membrane.

References

[1] Barber AJ, Lieth E. Agrin accumulates in the brain microvascular basal lamina during development of the blood-brain barrier. Dev Dyn 1997;208:62–74.
[2] Bowe MA, Fallon JR. The role of agrin in synapse formation. Annu Rev Neurosci 1995;18:443–62.
[3] Bowen DC, Sugiyama J, Ferns M, Hall ZW. Neural agrin activates a high-affinity receptor in C2 muscle cells that is unresponsive to muscle agrin. J Neurosci 1996;16:3791–7.
[4] Braak H, Braak E. Neuropathological staging of Alzheimer-related changes. Acta Neuropathol 1991;82:239–59.
[5] Buee L, Hof PR, Delacourte A. Brain microvascular changes in Alzheimer's disease and other dementias. Ann N Y Acad Sci 1997; 826:7–24.
[6] Campagna JA, Ruegg MA, Bixby JL. Evidence that agrin directly influences presynaptic differentiation at neuromuscular junctions in vitro. Eur J Neurosci 1997;9:2269–83.
[7] Castillo GM, Ngo C, Cummings J, Wight TN, Snow AD. Perlecan binds to the beta-amyloid proteins (A beta) of Alzheimer's disease, accelerates A beta fibril formation, and maintains A beta fibril stability. J Neurochem 1997;69:2452–65.
[8] Cohen NA, Kaufmann WE, Worley PF, Rupp F. Expression of agrin in the developing and adult rat brain. Neuroscience 1997;76:581–96.
[9] Davies P, Katzman R, Terry RD. Reduced somatostatin-like immunoreactivity in cerebral cortex from cases of Alzheimer disease and Alzheimer senile dementia. Nature 1980;288:279–80.
[10] Davies CA, Mann DM, Sumpter PQ, Yates PO. A quantitative morphometric analysis of the neuronal and synaptic content of the frontal

and temporal cortex in patients with Alzheimer's disease. J Neurol Sci 1987;78:151–64.
[11] de la Torre JC. Hemodynamic consequences of deformed microvessels in the brain in Alzheimer's disease. Ann N Y Acad Sci 1997; 26:826:75–91.
[12] Denzer AJ, Brandenberger R, Gesemann M, Chiquet M, Ruegg MA. Agrin binds to the nerve-muscle basal lamina via laminin. J Cell Biol 1997;137:671–83.
[13] Donahue JE, Berzin TM, Rafii MS, et al. Agrin in Alzheimer's disease: altered solubility and abnormal distribution within microvasculature and brain parenchyma. Proc Natl Acad Sci U S A 1999;96: 6468–72.
[14] Ferns M, Hoch W, Campanelli JT, Rupp F, Hall ZW, Scheller RH. RNA splicing regulates agrin-mediated acetylcholine receptor clustering activity on cultured myotubes. Neuron 1992;8:1079–86.
[15] Garcia VV, Alberca I, Borrasca AL. Factor VIII-related antigen in cerebrospinal fluid. Thromb Haemost 1983;49:142–3.
[16] Geddes JW, Monaghan DT, Cotman CW, Lott IT, Kim RC, Chui HC. Plasticity of hippocampal circuitry in Alzheimer's disease. Science 1985;230:1179–81.
[17] Halfter W. A heparan sulfate proteoglycan in developing avian axonal tracts. J Neurosci 1993;13:2863–73.
[18] Halfter W, Schurer B, Yip J, et al. Distribution and substrate properties of agrin, a heparan sulfate proteoglycan of developing axonal pathways. J Comp Neurol 1997;383:1–17.
[19] Halfter W, Dong S, Schurer B, Cole GJ. Collagen XVIII is a basement membrane heparan sulfate proteoglycan. J Biol Chem 1998; 273:25404–12.
[20] Hamos JE, DeGennaro LJ, Drachman DA. Synaptic loss in Alzheimer's disease and other dementias. Neurology 1989;39:355–61.
[21] Hilgenberg LG, Hoover CL, Smith MA. Evidence of an agrin receptor in cortical neurons. J Neurosci 1999;19:7384–93.
[22] Hoch W, Ferns M, Campanelli JT, Hall ZW, Scheller RH. Developmental regulation of highly active alternatively spliced forms of agrin. Neuron 1993;11:479–90.
[23] Kalman J, Juhasz A, Csaszar A, et al. Increased apolipoprotein E4 allele frequency is associated with vascular dementia in the Hungarian population. Acta Neurol Scand 1998;98:166–88.
[24] Khachaturian ZS. Diagnosis of Alzheimer's disease. Arch Neurol 1985;42:1097–1105.
[25] Kroger S, Horton SE, Honig LS. The developing avian retina expresses agrin isoforms during synaptogenesis. J Neurobiol 1996;29: 165–82.
[26] Larner AJ. The cortical neuritic dystrophy of Alzheimer's disease: nature, significance, and possible pathogenesis. Dementia 1995;6: 218–24.
[27] Lassmann H, Weiler R, Fischer P, et al. Synaptic pathology in Alzheimer's disease: immunological data for markers of synaptic and large dense-core vesicles. Neuroscience 1992;46:1–8.
[28] Lewczuk P, Reiber H, Ehrenreich H. Prothrombin in normal human cerebrospinal fluid originates from the blood. Neurochem Res 1998; 23:1027–30.
[29] Mcarron MO, Muir KW, Weir CJ, et al. The apolipoprotein E epsilon 4 allele and outcome in cerebrovascular disease. Stroke 1998;29: 1882–7.
[30] Narindrasorasak S, Lowery DE, Altman RA, Gonzalez–DeWhitt PA, Greenberg BD, Kisilevsky R. Characterization of high affinity binding between laminin and Alzheimer's disease amyloid precursor proteins. Lab Invest 1992;67:643–52.
[31] Nitkin RM, Smith MA, Magill C, et al. Identification of agrin, a synaptic organizing protein from Torpedo electric organ. J Cell Biol 1987;105:2471–8.
[32] O'Connor LT, Lauterborn JC, Gall CM, Smith MA. Localization and alternative splicing of agrin mRNA in adult rat brain: transcripts encoding isoforms that aggregate acetylcholine receptors are not restricted to cholinergic regions. J Neurosci 1994;14:1141–52.
[33] Perlmutter LS, Barron E, Saperia D, Chui HC. Association between vascular basement membrane components and the lesions of Alzheimer's disease. J Neurosci Res 1991;30:673–81.
[34] Perlmutter LS. Microvascular pathology and vascular basement membrane components in Alzheimer's disease. Mol Neurobiol 1994;9:33–40.
[35] Perry G, Siedlak SL, Richey P, et al. Association of heparan sulfate proteoglycan with the neurofibrillary tangles of Alzheimer's disease. J Neurosci 1991;11:3679–83.
[36] Reist NE, Magill C, McMahan UJ. Agrin-like molecules at synaptic sites in normal, denervated, and damaged skeletal muscles. J Cell Biol 1987;105:2457–69.
[37] Roses AD. The Alzheimer diseases. Curr Opin Neurobiol 1996;6: 644–50.
[38] Sims NR, Bowen DM, Allen SJ, et al. Presynaptic cholinergic dysfunction in patients with dementia. J Neurochem 1983;40:503–9.
[39] Small DH, Nurcombe V, Reed G, et al. A heparin-binding domain in the amyloid protein precursor of Alzheimer's disease is involved in the regulation of neurite outgrowth. J Neurosci 1994;14:2117–27.
[40] Small DH, Williamson T, Reed G, et al. The role of heparan sulfate proteoglycans in the pathogenesis of Alzheimer's disease. Ann N Y Acad Sci 1996;777:316–21.
[41] Smith MA, Yao YM, Reist NE, Magill C, Wallace BG, McMahan UJ. Identification of agrin in electric organ extracts and localization of agrin-like molecules in muscle and central nervous system. J Exp Biol 1987;132:223–30.
[42] Snow AD, Mar H, Nochlin D, et al. The presence of heparan sulfate proteoglycans in the neuritic plaques and congophilic angiopathy in Alzheimer's disease. Am J Pathol 1988;133:456–63.
[43] Snow AD, Sekiguchi R, Nochlin D, et al. An important role of heparan sulfate proteoglycan (Perlecan) in a model system for the deposition and persistence of fibrillar A beta-amyloid in rat brain. Neuron 1994;12:219–34.
[44] Tsen G, Halfter W, Kroger S, Cole GJ. Agrin is a heparan sulfate proteoglycan. J Biol Chem 1995;270:3392–9.
[45] Wallace BG. Agrin-induced specializations contain cytoplasmic, membrane, and extracellular matrix-associated components of the postsynaptic apparatus. J Neurosci 1989;9:1294–1302.
[46] Zhang P, Hirsch EC, Damier P, Duyckaerts C, Javoy–Agid F. c-fos protein-like immunoreactivity: distribution in the human brain and over-expression in the hippocampus of patients with Alzheimer's disease. Neuroscience 1992;46:9–21.